# Modular mathematical analysis of the control of flagellar $Ca^{2+}$-spike trains produced by CatSper and $Ca_V$ channels in sea urchin sperm

D.A.Priego-Espinosa[1], A.Darszon[2], A.Guerrero[2], A.L.González-Cota[3], T.Nishigaki[2], G.Martinez-Mekler[1,4,5,*], J.Carneiro[6,*]

[1] Instituto de Ciencias Físicas, Universidad Nacional Autónoma de México, 62210, Cuernavaca, Morelos, México

[2] Instituto de Biotecnología, Universidad Nacional Autónoma de México, 62210, Cuernavaca, Morelos, México

[3] Washington University School of Medicine, Department of Obstetrics and Gynecology. Center for Reproductive Health Sciences. 425 S Euclid Ave, St. Louis, MO 63110

[4] Centro de Ciencias de la Complejidad UNAM, CDMX, México

[5] Laboratoire de Physique Statistique de L'Ecole Normale Supérieure, 24 rue Lhomond, 75231 Paris, France.

[6] Instituto Gulbenkian de Ciência, Rua da Quinta Grande 6, 2780-156, Oeiras, Portugal

*Correspondence and requests for materials should be addressed to G.M.-M. or J.C. (e-mail: mekler@icf.unam.mx, jcarneir@igc.gulbenkian.pt)

# Supporting Information

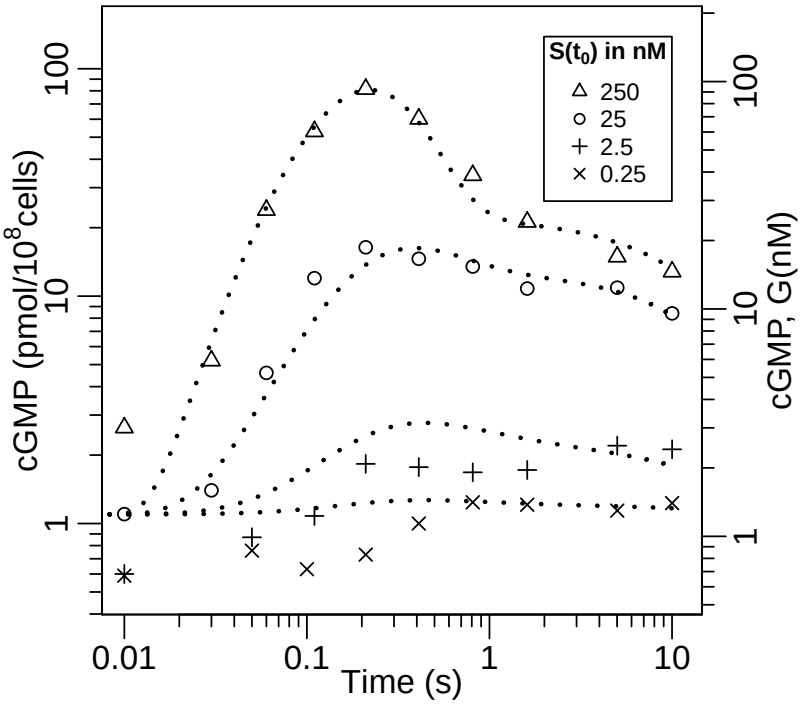


**Figure S1. Kinetics of intracellular cGMP concentration elicited by different SAP concentrations in bulk sperm populations**. (symbols; values read from graphs in[1]) and the corresponding model fitting using the upstream module components $\{S,R_H,R_L,G\}$. Plotted in log-log scale, it is shown data from different initial SAP stimuli (extracted from [1]); a particular symbol type is assigned to each SAP concentration, as indicated in the figure legend. Dotted lines correspond to rescaled single cell simulations after fitting the upstream module components.

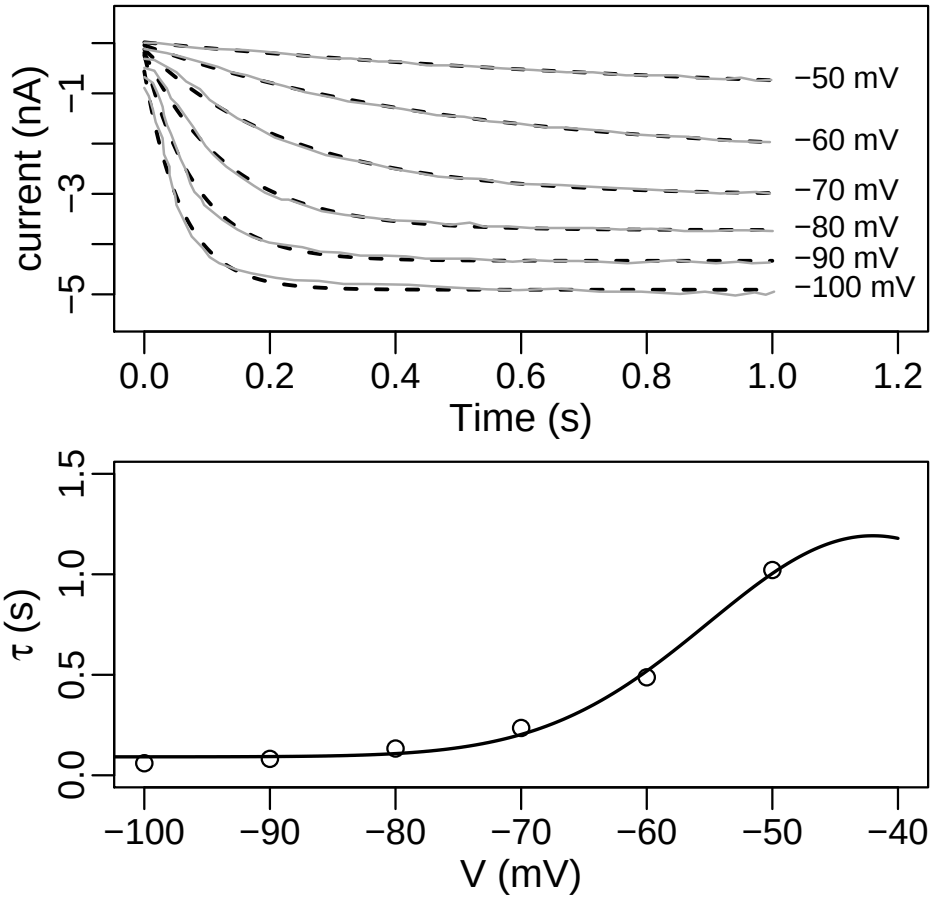


**Figure S2. Calibration of spHCN gating parameters**. In the upper panel, experimental traces of ionic currents measured by whole cell patch clamp technique in HEK cells expressing heterologously spHCN and loaded with photoactivatable cAMP analog, which in turn was uncaged by UV light. The set of currents correspond to different voltage pulses (indicated at the end of the trace). Data extracted from figure 4a of [2] (gray lines). Each trace was fitted to an an exponential function (black dashed lines) in order to estimate the characteristic activation time ($\tau$). In the lower pannel, the set of estimated characteristic times was fitted to a Gaussian function, which is our proposed form for the voltage-dependent characteristic time of spHCN gating (eq. 18).

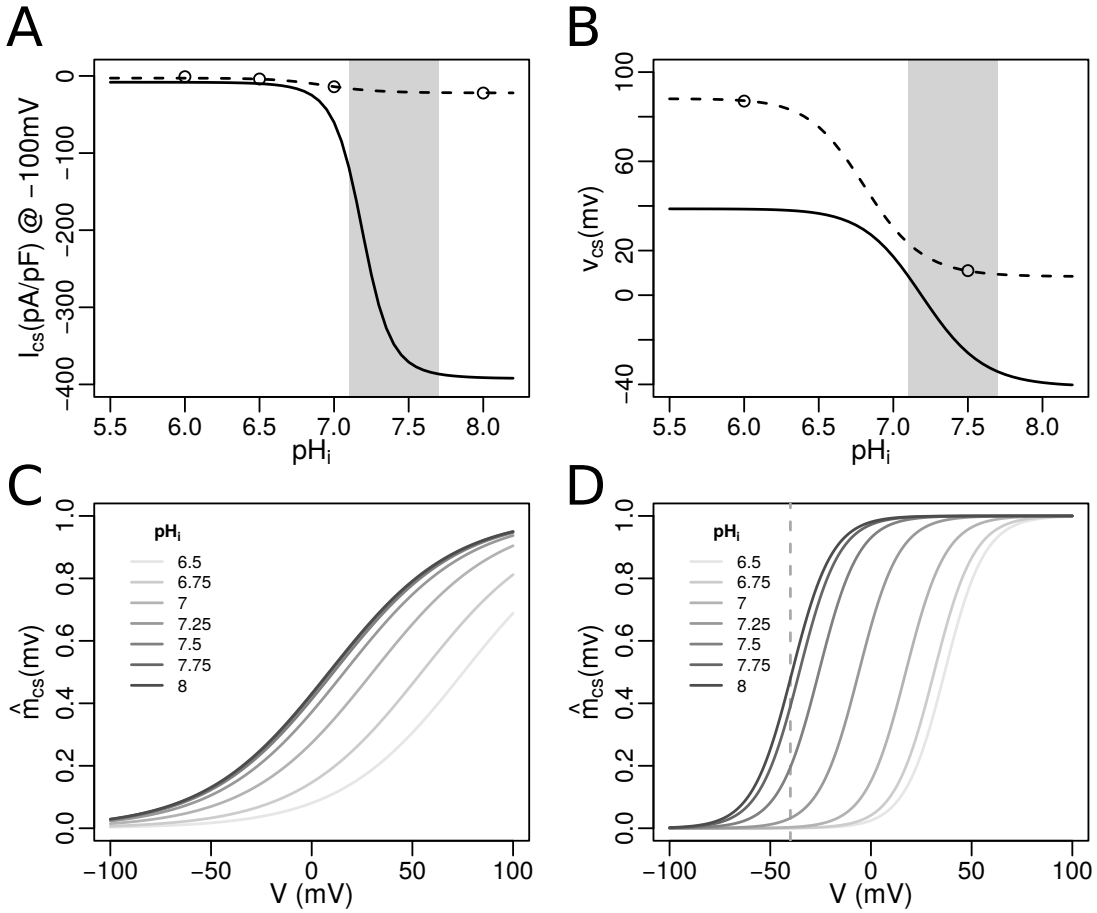


**Figure S3. Calibration of the CatSper's pH- and voltage-dependent gate**. In A and B, experimental data on mouse sperm (circles) are shown, along with model fittings (lines) related to the voltage- and $pH_i$-dependent gate variable in equilibrium, $\hat{m}_{cs}$. Model fittings in mouse and sea urchin cases are plotted with dashed and bold lines, respectively. The experimental data of A correspond to the current amplitude of divalent ions (symmetrical $Ba^{2+}$) produced by taking the holding voltage from 0 mV to −100 mV, under different $pH_i$ values, and measured by whole-cell patch-clamp in mouse sperm, (data extracted from Fig. 4c of [3]). Mouse data displayed in A and B were simultaneous fitted to the equations 34 and 31. To calibrate sea urchin's $\hat{m}_{cs}$, we took the parameters obtained with mouse data as a starting point and manually adjusted them, constraining that the $pH_i$ sensitivity should be within the physiological $pH_i$ response observed in sea urchin sperm (area marked in gray). C and D correspond to the G/V (conductance/voltage) curves of mouse and sea urchin CatSper, respectively, using the equation 30. In C, the parameters reported in [3] were used). In panel D, the resting membrane potential is indicated with a gray dashed line as reference. Taking into account that the S4 segment of CatSper voltage sensor domain has more positive charges in the sea urchin homologue protein that in the mammalian counterparts [4], we envisioned that its voltage sensitivity should be steeper. Thus, a 3-fold decrease was introduced to the voltage sensitivity parameter, $s_2$, as an initial guess. This last parameter has not been estimated in sea urchin due to the lack of patch-clamp measurements

## Supporting references


[1] U Benjamin Kaupp et al. "The signal flow and motor response controling chemotaxis of sea urchin sperm." In: *Nature cell biology* 5.2 (Feb. 2003), pp. 109–17. ISSN: 1465-7392. DOI: 10.1038/ncb915.

[2] Renate Gauss, Reinhard Seifert, and U Benjamin Kaupp. "Molecular identification of a hyperpolarization-activated channel in sea urchin sperm." In: *Nature* 393.6685 (June 1998), pp. 583–7. ISSN: 0028-0836. DOI: 10.1038/31248.

[3] Yuriy Kirichok, Betsy Navarro, and David E Clapham. "Whole-cell patch-clamp measurements of spermatozoa reveal an alkaline-activated Ca2+ channel." In: *Nature* 439.7077 (Feb. 2006), pp. 737–40. ISSN: 1476-4687. DOI: 10.1038/nature04417.

[4] Reinhard Seifert et al. "The CatSper channel controls chemosensation in sea urchin sperm". In: *The EMBO Journal* 34 (Dec. 2014), pp. 379–392. ISSN: 0261-4189. DOI: 10.15252/embj.201489376.